

Thermal emission from Isolated Neutron Stars and their surface magnetic field: going quadrupolar?

S. Zane,^a R. Turolla^b

^a*MSSL, University College of London, Holmbury St Mary, Surrey, RH5 6NT, UK*

^b*Dept. of Physics, University of Padua, via Marzolo 8, Padua, Italy*

Abstract

In the last few years considerable observational resources have been devoted to study the thermal emission from isolated neutron stars. Detailed *XMM* and *Chandra* observations revealed a number of features in the X-ray pulse profile, like asymmetry, energy dependence, and possible evolution of the pulse profile over a time scale of months or years. Here we show that these characteristics may be explained by a patchy surface temperature distribution, which is expected if the magnetic field has a complex structure in which higher order multipoles contribute together with the dipole. We reconsider these effects from a theoretical point of view, and discuss their implications to the observational properties of thermally emitting neutron stars.

Key words: Neutron Stars, Magnetic Field, X-ray: Pulsations, Radiative Transfer

PACS: 97.60.Jd, 97.60.Gb, 97.10.Ex, 97.10.Sj, 5.85.Nv

1 Introduction

The seven X-ray dim isolated neutron stars (XDINSs) discovered so far (see e.g. Treves et al. 2000, Motch 2001 for a review) offer an unprecedented opportunity to confront present models of neutron star (NS) surface emission with observations. These objects play a key role in compact objects astrophysics being the only sources in which we can have a clean view of the compact star surface. In particular, when pulsations and/or long term variations are detected we can study the shape and evolution of the pulse profile of the thermal emission and obtain information about the thermal and magnetic map of the star surface. So far, X-ray pulsations have been detected in four XDINSs, with periods in the range 3–11 s. In each of the four cases the pulsed fraction is relatively large ($\sim 12\% – 35\%$) and, counter-intuitively, the softness ratio

is maximum at the pulse maximum (Cropper et al. 2001, Haberl et al. 2003). Spectral lines have been detected in the soft X-rays and the line parameters may change with spin pulse. In addition, often the X-ray light curves appears to be slightly asymmetric and a gradual, long term evolution in both the X-ray spectrum and the pulse profile of the second most luminous source, RX J0720.4-3125 has been recently discovered (De Vries et al. 2004).

All these new findings represent a challenge for conventional atmospheric models: the properties of the observed pulse profiles (large pulsed fraction, skewness, and possibly time variations) cannot be explained by assuming that the thermal emission originates at the NS surface if the thermal distribution is induced by a simple core-centered dipolar magnetic field. On the other hand, it has been realized long ago that two effects can contribute at least to achieve relatively large pulsed fraction (up to 20%) : 1) radiative beaming (Pavlov et al. 1994) and 2) the presence of quadrupolar components in the magnetic field (Page and Sarmiento 1996). Here we present magnetized atmospheric models computed assuming a quadrupolar magnetic field geometry and show how they can account for some of the general characteristics of the observed X-ray lightcurves (see Zane and Turolla 2004, in preparation for further details).

2 Getting to grips with the neutron star surface

2.1 Computing the light curve

In order to compute the phase-dependent spectrum emitted by a cooling NS as seen by a distant observer, we basically perform three steps. First, we assume that the star magnetic field possesses a core-centered dipole+quadrupole topology, $\mathbf{B} = \mathbf{B}_{dip} + \mathbf{B}_{quad}$, where $\mathbf{B}_{quad} = \sum_{i=0}^4 q_i \mathbf{B}_{quad}^{(i)}$. The polar components of \mathbf{B}_{dip} and of the five generating vectors $\mathbf{B}_{quad}^{(i)}$ are reported in Page and Sarmiento (1996). The NS surface temperature distribution is then computed using the simple expression $T_s = T_p |\cos \alpha|^{1/2}$, where T_p is the polar temperature and α is the angle between the field and the radial direction, $\cos \alpha = \mathbf{B} \cdot \mathbf{n}$. Second, we compute the local spectrum emitted by each patch of the star surface by using fully ionized, magnetized hydrogen atmosphere models.¹ Besides surface gravity, this depends on both the surface temperature T_s and magnetic field, either its strength and orientation with respect to the local normal. We introduce a (θ, ϕ) mesh which divides the star surface into a given number of patches. The atmospheric structure and radiative transfer are then computed locally by approximating each atmospheric patch with a plane parallel slab.

¹ We caveat that partial ionization effects are not included in our work. Bound atoms and molecules can affect the results, changing the radiation properties at relatively low T and high B (Potekhin et al. 2004).

Third, we collect the contributions of surface elements which are “in view” at different rotation phases (see Pechenick et al. 1983, Lloyd et al. 2003). We take the neutron star to be spherical (mass M , radius R) and rotating with constant angular velocity $\omega = 2\pi/P$, where P is the period. Since XDINs are slow rotators ($P \approx 10$ s), we can describe the space-time outside the NS in terms of the Schwarzschild geometry. Under these assumptions, for a fixed polar temperature, dipolar field strength and surface gravity M/R , the computed light curve depends on seven parameters: $b_i \equiv q_i/B_{dip}$ ($i = 0, \dots, 4$), the angle χ between line of sight and spin axis, and the angle ξ between magnetic dipole and spin axis.

2.2 Studying light curves as a population and fitting the observed pulse shapes

Given this multidimensional dependence, an obvious question is whether or not we can identify some possible combinations of the independent parameters that are associated to particular features observed in the pulse shape. Particularly promising for a quantitative classification is a tool called principal components analysis (PCA), which is concerned with finding the minimum number of linearly independent variables z_p (called the principal components, PCs) needed to recreate a data set. In order to address this issue, we divided the phase interval ($0 \leq \gamma \leq 1$) in 32 equally spaced bins, and we computed a population of 78000 light curves by varying χ , ξ and b_i ($i = 0, \dots, 4$). By applying a PCA, we found that each light curve can be reproduced by using only the first ~ 20 more significant PCs and that the first four (three) PCs account for 85% (72%) of the total variance. However, due to the strong non-linearity, we find so far difficult to relate the PCs to physical variables.

Nevertheless, the PCA can be regarded as an useful method to provide a link between the various light curves, since models “close” to each other in the PCs space have similar characteristics. From the PCA we obtain the matrix C_{ij} such that $z_i \equiv C_{ij}y_j$, where y_j is the observed X-ray intensity at phase γ_j and z_i is the i -th PC. Therefore, we can compute the PCs corresponding to each observed light curve and search the models population for the nearest solution in the PCs space (see fig. 1, left). This in turn provides us a good trial solution, which can be used as a starting point for a numerical fit. The quadrupolar components and viewing angles are treated as free parameters while the polar values of T_p and B_{dip} are fixed and must fall in the domain spanned by our atmosphere model archive.² Our preliminary results are illustrated in Fig. 1, 2, and 3, and refer to $B_{dip} = 6 \times 10^{12}$ G, $\log T_p(\text{K}) = 6.1 - 6.2$.

² In general this will not contain the exact values inferred from spectral observations of XDINSs. However, we have checked that a fit (albeit with different values of the quadrupolar field) is possible for different combinations of B_{dip} and T_p in the range of interest.

3 Summary of results

As we can see from Fig. 1, 2 and 3, the broad characteristics of all the XDINS light curves observed so far are reproduced when allowing for a combination of quadrupolar magnetic field components and viewing angles. However, although in all cases a fit exists, we find that in general it may be not unique. This model has not a "predictive" capacity in providing the exact values of the magnetic field components and viewing angles: this is why we do not fit for all the parameters in a proper sense and we do not derive parameter uncertainties or confidence levels. The goal is instead to show that there exist at least one (and more probably more) combination of parameters that can explain the observed pulse shapes, while this is not possible assuming a pure dipole configuration. In the case of RX J0720.4-3125, preliminary results show that the pulse variation observed between rev.78 and rev.711 can not be explained by a change in viewing angle only (as it should be if NS precession is invoked, de Vries et al. 2004) or magnetic field only. Instead, a change in all quantities (quadrupolar components and viewing angles) is needed.³ Aim of our future work is to reduce the degeneracy either by performing a more detailed statistical analysis on the models population and by refining the best fits solutions by using information from the light curves observed in different color bands and/or from the spectral line variations with spin pulse.

References

Cropper, M., Zane, S., Ramsay, G., et al. Modelling the spin pulse profile of the isolated neutron star RX J0720.4-3125 observed with XMM-Newton. *Astron. & Astrophys.*, 365, L302-L307, 2001

de Vries, C.P., Vink, J., Mendez, M. et al. Long-term variability in the X-ray emission of RX J0720.4-3125. *Astron. & Astrophys.*, 415, L31-L34, 2004

Geppert, U., Rheinhardt, M., Gil, J. Spot-like structures of neutron star surface magnetic fields. *Astron. & Astrophys.*, 412, L33-L36, 2003

Haberl, F., Schwope, A.D., Hambaryan, V., et al. A broad absorption feature in the X-ray spectrum of the isolated neutron star RBS1223 (1RXS J130848.6+212708). *Astron. & Astrophys.*, 403, L19-L23, 2003

Haberl, F., Motch, C., Zavlin, V.E., et al. The isolated neutron star X-ray

³ How to produce field variations on such a short timescale needs to be addressed in more detail and, at present, no definite conclusion can be drawn. For instance, a change of the magnetic field structure and strength on a timescale of years may be conceivable if the surface field is small scaled (Geppert et al. 2003). In this case, even small changes in the inclination between line of sight and local magnetic field axis may cause significant differences in the "observed" field strength.

pulsars RX J0420.0-5022 and RX J0806.4-4123: New X-ray and optical observations. *Astron. & Astrophys.*, 424, 635-645, 2004

Lloyd, D.A., Perna, R., Slane, P. et al. A pulsar-atmosphere model for PSR 0656+14, *astro-ph/0306235*, 2003.

Motch, C. Isolated neutron stars discovered by ROSAT, in: N.E. White, G. Malaguti, and G.G.C. Palumbo (Eds.), *X-ray Astronomy: Stellar Endpoints, AGN, and the Diffuse X-ray Background*. NY: American Institute of Physics. AIP Conference Proceedings, Vol. 599, pp. 244-253, 2001.

Pavlov, G.G., Shibanov, Yu.A., Ventura, J. et al. Model atmospheres and radiation of magnetic neutron stars: Anisotropic thermal emission. *Astron. & Astrophys.*, 289, 837-845, 1994

Page, D., Sarmiento, A. Surface Temperature of a Magnetized Neutron Star and Interpretation of the ROSAT Data. II. *Astr. J.*, 473, 1067-1078, 1996

Pechenick, K.R., Ftaclas, C., Cohen, J.M. Hot spots on neutron stars - The near-field gravitational lens. *Astr. J.*, 274, 846-857, 1983

Potekhin, A. Y., Lai, D., Chabrier, G., et al., Electromagnetic Polarization in Partially Ionized Plasmas with Strong Magnetic Fields and Neutron Star Atmosphere Models, *ApJ*, 612, 1034, 2004

Treves, A., Turolla, R., Zane, S., et al. Isolated Neutron Stars: Accretors and Coolers. *PASP*, 112, 297-314, 2000

- Fig. 1. Left: The computed population of 78000 light curves plotted against the first 3 principal components. Axis are arbitrary; yellow symbols mark the position of the EPIC-PN light curves of the XDINSs (see next captions for references; both rev. 78 and rev. 711 are shown for RX J0720.4-3125), red symbols mark the light curves computed assuming a pure dipolar field. The PCs representation (limited to the first three PCs, which alone account for the 72% of the total variance) of the observed light curves falls within the domain spanned by the quadrupolar model representations; this is why at least one fitting solution can be found. Right: Fit of the EPIC-PN (0.12-0.7 keV) smoothed light curve of RX J0420.0-5022 (Haberl et al. 2004, rev. 570). Dashed line: trial solution as inferred from the closest model in the PCs space; solid line: best fit solution. The best fit parameters are: $b_0 = -0.48$, $b_1 = 0.02$, $b_2 = -0.25$, $b_3 = 0.35$, $b_4 = -0.20$, $\xi = 39.9^\circ$, $\chi = 91.2^\circ$.
- Fig. 2. Same as in the right panel of Fig. 1 for two further INSs. Left: Fit of the EPIC-PN (0.12-1.2 keV) light curve of RX J0806.4-4123 (rev. 618, Haberl et al. 2004). Here: $b_0 = 0.39$, $b_1 = -0.37$, $b_2 = 0.12$, $b_3 = -0.13$, $b_4 = 0.49$, $\xi = 0.0^\circ$, $\chi = 59.2^\circ$. Right: fit of the EPIC-PN (0.12-0.5 keV) light curve of RBS 1223 (rev. 561, Haberl et al. 2003). Here: $b_0 = 0.21$, $b_1 = -0.02$, $b_2 = 0.59$, $b_3 = 0.53$, $b_4 = 0.50$, $\xi = 0.0^\circ$, $\chi = 95.1^\circ$.
- Fig. 3. Same as in the right panel of Fig. 1 for the fit of two EPIC-PN (0.12-1.2 keV) light curves of RX J0720.4-3125 (both from De Vries et al. 2004). Left (rev. 78): $b_0 = 0.36$, $b_1 = 0.43$, $b_2 = -0.16$, $b_3 = -0.16$, $b_4 = -0.39$, $\xi = 0.0^\circ$, $\chi = 68.1^\circ$. Right (rev. 711): $b_0 = 0.45$, $b_1 = 0.49$, $b_2 = -0.06$, $b_3 = -0.08$, $b_4 = -0.26$, $\xi = 0.0^\circ$, $\chi = 87.6^\circ$.

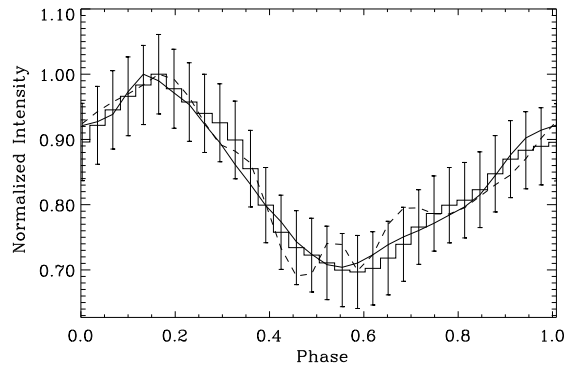
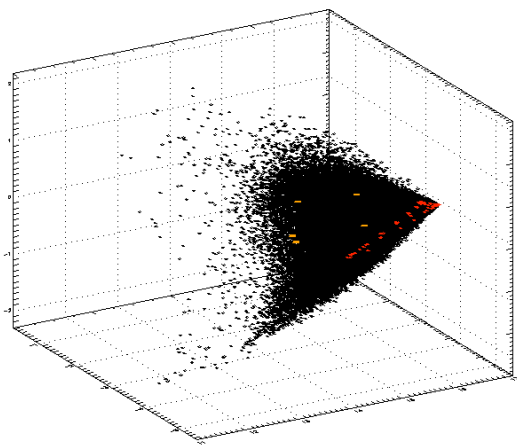


Fig. 1.

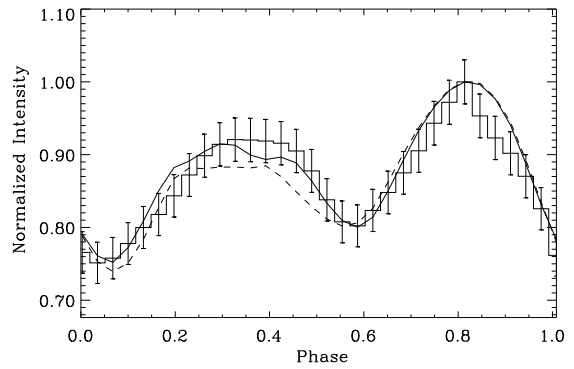
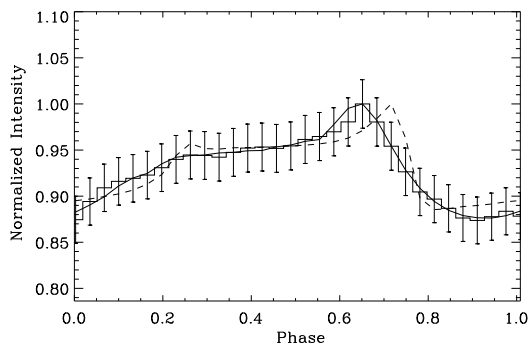


Fig. 2.

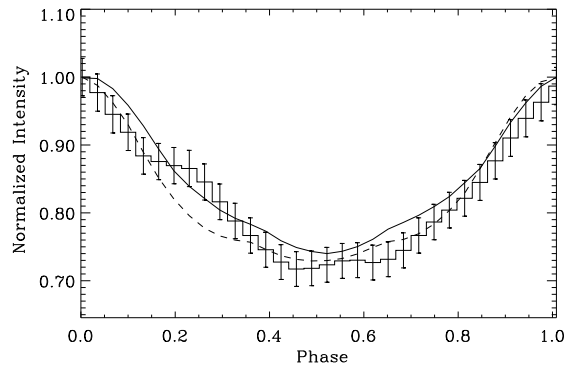
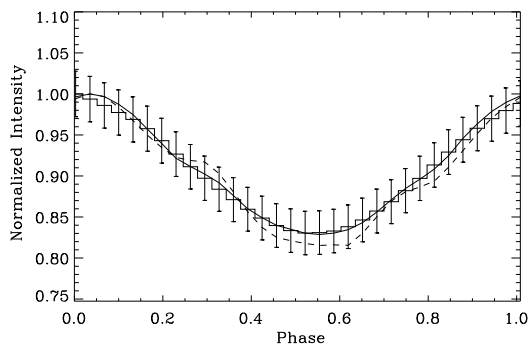


Fig. 3.